Molecular Biology of the Cell
Vol. 18, 4885–4898, December 2007

Scd5p Mediates Phosphoregulation of Actin and Endocytosis by the Type 1 Phosphatase Glc7p in Yeast[D] [V]

Guisheng Zeng,* Bo Huang,* Suat Peng Neo, Junxia Wang, and Mingjie Cai

Institute of Molecular and Cell Biology, Singapore 138673, Republic of Singapore

Submitted June 26, 2007; Revised September 5, 2007; Accepted September 13, 2007
Monitoring Editor: Sandra Schmid

Pan1p plays essential roles in both actin and endocytosis in yeast. It interacts with, and regulates the function of, multiple endocytic proteins and actin assembly machinery. Phosphorylation of Pan1p by the kinase Prk1p down-regulates its activity, resulting in disassembly of the endocytic vesicle coat complex and termination of vesicle-associated actin polymerization. In this study, we focus on the mechanism that acts to release Pan1p from phosphorylation inhibition. We show that Pan1p is dephosphorylated by the phosphatase Glc7p, and the dephosphorylation is dependent on the Glc7p-targeting protein Scd5p, which itself is a phosphorylation target of Prk1p. Scd5p links Glc7p to Pan1p in two ways: directly by interacting with Pan1p and indirectly by interacting with the Pan1p-binding protein End3p. Depletion of Glc7p from the cells causes defects in cell growth, actin organization, and endocytosis, all of which can be partially suppressed by deletion of the *PRK1* gene. These results suggest that Glc7p antagonizes the activity of the Prk1p kinase in regulating the functions of Pan1p and possibly other actin- and endocytosis-related proteins.

INTRODUCTION

Clathrin-mediated endocytosis involves elaborate spatial and temporal recruitment of endocytic adaptors, coat elements, and actin cytoskeletal factors in yeast and mammalian cells (Kaksonen *et al*., 2003; Merrifield, 2004; Kaksonen *et al*., 2005, 2006). Some four protein modules have been recently suggested to be responsible for driving distinct stages of endocytosis in yeast (Kaksonen *et al*., 2005). The coat module consists of proteins that assemble early at the endocytic sites to initiate coat formation. The WASP/Myosin module activates the Arp2/3-mediated actin polymerization to induce membrane invagination. The actin module organizes actin filaments into a branched meshwork to facilitate coat movement, and the amphiphysin module functions in vesicle scission. The released vesicles are thought to be propelled into the cytosol by actin polymerization, accompanied by the disassembly of the coat complex (Kaksonen *et al*., 2006).

The essential yeast protein Pan1p plays a central role in coat formation by interacting with multiple coat proteins, including End3p, Sla1/2p, Yap1801/2p, and Ent1/2p (Tang *et al*., 1997; Wendland and Emr, 1998; Wendland *et al*., 1999; Tang *et al*., 2000; Toshima *et al*., 2007). Pan1p also possesses the ability to activate the Arp2/3 complex, and may cooperate with other nucleation-promoting factors, such as Las17p and Myo5p, to initiate actin assembly at endocytic sites (Duncan *et al*., 2001; Sun *et al*., 2006). Furthermore, Pan1p can directly bind to actin filaments via its WH2-like region (Toshima *et al*., 2005), thereby providing an anchor point for actin meshwork to associate with the endocytic coat. The functions of Pan1p are under a negative regulation by the serine/threonine kinase Prk1p (Zeng and Cai, 1999; Zeng *et al*., 2001; Toshima *et al*., 2005). Phosphorylation of Pan1p by Prk1p on the LxxQxTG motifs disrupts the Pan1p–Sla1p complex (Zeng *et al*., 2001), and prevents Pan1p from associating with actin filaments and activating the Arp2/3 complex (Toshima *et al*., 2005). This regulation is presumably to allow vesicles to be uncoated and uncoupled from the actin meshwork after they are internalized. Compared with the progressing studies of the regulation of Pan1p by phosphorylation, very little is known about how Pan1p regains its activity after phosphoinhibition.

The type 1 protein phosphatase (PP1) of *Saccharomyces cerevisiae*, Glc7p, has been shown to be involved in a diversity of cellular processes such as glycogen metabolism (Feng *et al*., 1991), translational control (Wek *et al*., 1992), glucose repression (Tu and Carlson, 1994), cell cycle progression (Hisamoto *et al*., 1994), and chromosome segregation (Francisco *et al*., 1994). The ability of Glc7p to perform such diverse functions stems presumably from its interactions with various targeting factors that direct the phosphatase to different substrates and/or sites of activity. For example, Reg1p binds and targets Glc7p to its substrates in the glucose repression regulatory pathway (Tu and Carlson, 1995). A group of Glc7p-interacting proteins have been identified by Tu *et al*. (1996) using the two-hybrid protein interaction assay. One of them, Scd5p, has recently been confirmed to interact with Glc7p in vivo (Chang *et al*., 2002). Similar to Pan1p, Scd5p is also a phosphorylation target of Prk1p, and has been shown to function in cortical actin organization and endocytosis (Henry *et al*., 2002; Henry *et al*., 2003; Huang *et al*., 2003). There is a pressing need, therefore, to ascertain whether Glc7p is involved in the regulation of actin and endocytosis through its interaction with Scd5p.

In this study, we demonstrate that Glc7p functions antagonistically to Prk1p in modulating the phosphorylation status of Pan1p in vivo. Scd5p is a critical factor in determining

This article was published online ahead of print in *MBC in Press* (http://www.molbiolcell.org/cgi/doi/10.1091/mbc.E07–06–0607) on September 26, 2007.

[D] [V] The online version of this article contains supplemental material at *MBC Online* (http://www.molbiolcell.org).

* These authors contributed equally to this work.

Address correspondence to: Mingjie Cai (mcbcaimj@imcb.a-star.edu.sg).

Table 1. Yeast strains used in this study

Strain	Genotype
W303-1A	*MAT***a** *ade2-1 trp1-1 can1-100 leu2-3,112 his3-11,15 ura3-1*
W303-1B	*MATα ade2-1 trp1-1 can1-100 leu2-3,112 his3-11,15 ura3-1*
SFY526	*MAT***a** *ade2-101 trp1-901 can^r leu2-3,112 his3-200 ura3-52 lys2-801 gal4-542 gal80-538 URA3::GAL1-lacZ*
YMC422	*MAT***a** *ade2-1 trp1-1 can1-100 leu2-3,112 his3-11,15 ura3-1 pan1-4*
YMC441	*MAT***a** *ade2-1 trp1-1 can1-100 leu2-3,112 his3-11,15 ura3-1 pan1::PAN1-Myc-URA3*
YMC446	*MATα ade2-1 trp1-1 can1-100 leu2-3,112 his3-11,15 ura3-1 scd5-1 (scd5::SCD5$^{PBM2\Delta}$-LEU2)*
YMC448	*MATα ade2-1 trp1-1 can1-100 leu2-3,112 his3-11,15 ura3-1 scd5::SCD5-HA-LEU2*
YMC449	*MATα ade2-1 trp1-1 can1-100 leu2-3,112 his3-11,15 ura3-1 scd5::SCD5^{AAA}-HA-LEU2*
YMC471	*MATα ade2-1 trp1-1 can1-100 leu2-3,112 his3-11,15 ura3-1 scd5::SCD5-HA-LEU2 pan1::PAN1-Myc-URA3*
YMC472	*MATα ade2-1 trp1-1 can1-100 leu2-3,112 his3-11,15 ura3-1 scd5-1 pan1-4* pPAN1-316
YMC473	*MATα ade2-1 trp1-1 can1-100 leu2-3,112 his3-11,15 ura3-1 scd5::SCD5^{AAA}-HA-LEU2 pan1::PAN1-Myc-URA3*
YMC474	*MAT***a** *ade2-1 trp1–1 can1–100 leu2–3,112 his3–11,15 ura3–1 end3*Δ*::HIS3*
YMC475	*MAT***a** *ade2–1 trp1–1 can1–100 leu2–3,112 his3–11,15 ura3–1 scd5–1 end3*Δ*::HIS3* pEND3–316
YMC476	*MAT***a** *ade2-1 trp1-1 can1-100 leu2-3,112 his3-11,15 ura3-1 end3*Δ*::HIS3 scd5::SCD5-HA-LEU2*
YMC477	*MAT***a** *ade2-1 trp1-1 can1-100 leu2-3,112 his3-11,15 ura3-1 prk1*Δ*::HIS3*
YMC478	*MAT***a** *ade2-1 trp1-1 can1-100 leu2-3,112 his3-11,15 ura3-1 prk1*Δ*::HIS3 pan1::PAN1-Myc-URA3*
YMC479	*MATα ade2-1 trp1-1 can1-100 leu2-3,112 his3-11,15 ura3-1 scd5-1 pan1::PAN1-Myc-URA3*
YMC480	*MAT***a** *ade2-1 trp1-1 can1-100 leu2-3,112 his3-11,15 ura3-1 end3*Δ*::HIS3 pan1::PAN1-Myc-URA3*
YMC481	*MAT***a** *ade2-1 trp1-1 can1-100 leu2-3,112 his3-11,15 ura3-1 glc7::GLC7-HA-LEU2*
YMC482	*MAT***a** *ade2-1 trp1-1 can1-100 leu2-3,112 his3-11,15 ura3-1 pan1::PAN1-Myc-URA3 glc7::GLC7^{T152K}-HA-LEU2*
YMC483	*MAT***a** *ade2-1 trp1-1 can1-100 leu2-3,112 his3-11,15 ura3-1 pan1::PAN1-Myc-TRP1*
YMC484	*MAT***a** *ade2-1 trp1-1 can1-100 leu2-3,112 his3-11,15 ura3-1 pan1::PAN1-Myc-TRP1 glc7-td (glc7::GLC7-td-URA3)*
YMC485	*MAT***a** *ade2-1 trp1-1 can1-100 leu2-3,112 his3-11,15 ura3-1 pan1::PAN1-Myc-TRP1 glc7-ntd (glc7::GLC7-ntd-URA3)*
YMC486	*MAT***a** *ade2-1 trp1-1 can1-100 leu2-3,112 his3-11,15 ura3-1 prk1*Δ*::TRP1*
YMC487	*MATα ade2-1 trp1-1 can1-100 leu2-3,112 his3-11,15 ura3-1 scd5*Δ*::HIS5* pSCD5-HA-316
YMC488	*MATα ade2-1 trp1-1 can1-100 leu2-3,112 his3-11,15 ura3-1 prk1*Δ*::TRP1 scd5*Δ*::HIS5* pSCD5-HA-316
YMC489	*MATα ade2-1 trp1-1 can1-100 leu2-3,112 his3-11,15 ura3-1 scd5::SCD5$^{PBM2\Delta}$-HA-LEU2*
YMC490	*MATα ade2-1 trp1-1 can1-100 leu2-3,112 his3-11,15 ura3-1 scd5*Δ*::HIS5* pSCD5-HA-316 *glc7::GLC7^{T152K}-Myc-LEU2*
YMC491	*MAT***a** *ade2-1 trp1-1 can1-100 leu2-3,112 his3-11,15 ura3-1 scd5::SCD5-Myc-TRP1*
YMC492	*MAT***a** *ade2-1 trp1-1 can1-100 leu2-3,112 his3-11,15 ura3-1 scd5::SCD5-Myc-TRP1 glc7-ntd (glc7::GLC7-ntd-URA3)*
YMC493	*MAT***a** *ade2-1 trp1-1 can1-100 leu2-3,112 his3-11,15 ura3-1 scd5::SCD5-Myc-TRP1 glc7-td (glc7::GLC7-td-URA3)*
YMC494	*MAT***a** *trp1-1 leu2-3,112 his3 ura3 pan1::PAN1-GFP-HIS3MX*
YMC495	*MAT***a** *ade2-1 trp1-1 can1-100 leu2-3,112 his3-11,15 ura3-1 prk1::PRK1-GFP-LEU2*
YMC496	*MAT***a** *ade2-1 trp1-1 can1-100 leu2-3,112 his3-11,15 ura3-1 scd5::SCD5-GFP-HIS3MX*
YMC497	*MAT***a** *ade2-1 trp1-1 can1-100 leu2-3,112 his3-11,15 ura3-1 pan1::PAN1-CFP-TRP1 prk1::PRK1-GFP-LEU2*
YMC498	*MAT***a** *ade2-1 trp1-1 can1-100 leu2-3,112 his3-11,15 ura3-1 pan1::PAN1-CFP-TRP1 scd5::SCD5-GFP-HIS3MX*
YMC499	*MATα ade2-1 trp1-1 can1-100 leu2-3,112 his3-11,15 ura3-1 glc7-ntd (glc7::GLC7-ntd-URA3)*
YMC500	*MATα ade2-1 trp1-1 can1-100 leu2-3,112 his3-11,15 ura3-1 glc7-td (glc7::GLC7-td-URA3)*
YMC501	*MATα ade2-1 trp1-1 can1-100 leu2-3,112 his3-11,15 ura3-1 prk1*Δ*::HIS3 glc7-td (glc7::GLC7-td-URA3)*
YMC502	*MATα ade2-1 trp1-1 can1-100 leu2-3,112 his3-11,15 ura3-1 scd5::SCD5^{AAA}-HA-LEU2 pan1::PAN1-GFP-HIS3MX*

the phosphorylation status of Pan1p, as it serves not only as a Glc7p targeting factor but also as a switch in phosphorylation of Pan1p. These findings provide new insight into the mechanism that operates in the cycle of phosphoregulation of actin-driven endocytosis in yeast.

MATERIALS AND METHODS

Strains, Plasmids, and General Methods

Yeast strains and plasmids used in this study are listed in Table 1 and 2, respectively. Yeast cells were grown in standard yeast extract-peptone-dextrose (YEPD) or synthetic complete (SC) medium lacking appropriate amino acids for plasmid maintenance. In experiments requiring the expression of genes under the *GAL1* promoter, raffinose instead of dextrose was used as the carbon source and galactose was later added for *GAL1* induction. To maintain the growth of *glc7-td*, *glc7-ntd*, and *prk1*Δ *glc7-td* mutants, $CuSO_4$ was added to the medium at a final concentration of 0.1 mM. Mutations on Scd5p (PBM2Δ, AAA, and EEE) and Glc7p (T152K and ntd) were generated by polymerase chain reaction (PCR) mutagenesis. Strains YMC422, YMC441, YMC446, YMC448, and YMC449 were generated as described previously (Zeng and Cai, 1999; Zeng *et al*., 2001; Huang *et al*., 2003). Gene deletions in YMC474, YMC477, YMC486, and YMC487 were created by integrating a *HIS3*, *TRP1*, or *Schizosaccharomyces pombe HIS5* selection cassette to replace the chromosomal loci. Crosses of YMC446 with YMC422 containing pPAN1-316, YMC446 with YMC474 containing pEND3-316, YMC486 with YMC487, and DDY3063 (Kaksonen *et al*., 2005) with W303-1A, followed by sporulation and dissection, produced YMC472, YMC475, YMC488, and YMC494, respectively. The C-terminal green fluorescent protein (GFP)-fused *SCD5* in YMC496 and YMC498 were generated by the PCR-targeting method as described previously (Wach *et al*., 1997). Other strains were generated by integrating various linearized plasmids into corresponding host cells, respectively. Bacterial strains DH5α and BL21 were grown on standard medium supplemented with 100 μg/ml ampicillin to maintain plasmids. Genetic and recombinant DNA manipulations were performed according to standard techniques.

Protein Extraction, Immunoprecipitation, and Immunoblotting

Yeast extracts were prepared by either glass beads method or trichloroacetic acid (TCA) precipitation method as described previously (Tang *et al*., 1997; Huang *et al*., 2003). Immunoprecipitation and immunoblotting followed the published procedure (Tang *et al*., 1997) with slight modifications. The beads-conjugated anti-hemagglutinin (HA) or anti-Myc polyclonal antibodies (Santa Cruz Biotechnology, Santa Cruz, CA) were used to immunoprecipitate epitope-tagged proteins. For immunoblotting of precipitated proteins, monoclonal anti-HA or anti-Myc (clone 12CA5 and 9E10, respectively; Roche Applied Science, Indianapolis, IN), rabbit anti-phosphothreonine (anti-PThr; Zymed Laboratories, San Francisco, CA), or rabbit anti-G6PDH (Sigma-Aldrich, St. Louis, MO) antibodies were used as required. Horseradish peroxidase-conjugated goat anti-mouse or anti-rabbit antibodies (GE Healthcare, Chalfont St. Giles, United Kingdom) were used together with the ECL system (GE Healthcare) to visualize the antibody–antigen complex. Treatment of immunoprecipitates with calf intestinal alkaline phosphatase (CIP) was performed as described previously (Zeng and Cai, 1999). To increase the basal level of in vivo phosphorylated Scd5p, cells with locus-expressed Scd5-HA were incubated with the phosphatase inhibitor cocktail (10 μM sodium flu-

Table 2. Plasmid constructs used in this study

Construct	Description
pSCD5-N-BD	DNA fragment encoding Scd5p (1-534 amino acids [aa]) was cloned into pGBKT7
pSCD5-C-BD	DNA fragment encoding Scd5p (535-872 aa) was cloned into pGBKT7
pSCD5-N1-BD	DNA fragment encoding Scd5p (1-301 aa) was cloned into pGBKT7
pSCD5-N2-BD	DNA fragment encoding Scd5p (302-534 aa) was cloned into pGBKT7
pPAN1-LR1-AD	DNA fragment encoding Pan1p (1-385 aa) was cloned into pGADT7
pPAN1-LR2-AD	DNA fragment encoding Pan1p (384-713 aa) was cloned into pGADT7
pPAN1-CC-AD	DNA fragment encoding Pan1p (641-1310 aa) was cloned into pGADT7
pPAN1-PP-AD	DNA fragment encoding Pan1p (1239-1480 aa) was cloned into pGADT7
pPAN1-314	The *PAN1* gene was generated by PCR and cloned into pRS314 (Tang *et al.*, 2000)
pPAN1-316	The *PAN1* gene was generated by PCR and cloned into pRS316 (Tang *et al.*, 2000)
pGEX-LR2	GST-LR2; DNA fragment encoding Pan1p (384-713 aa) was cloned into pGEX-4T-1
pET-SCD5-N1	His-SCD5-N1; DNA fragment encoding Scd5p (1-301 aa) was cloned into pET-32a
pET-SCD5-N2	His-SCD5-N2; DNA fragment encoding SCD5p (302-534 aa) was cloned into pET-32a
pET-SCD5-C	His-SCD5-C; DNA fragment encoding SCD5p (535-872 aa) was cloned into pET-32a
pEND3-316	The *END3* gene was generated by PCR and cloned into pRS316
pEND3-314	The *END3* gene was generated by PCR and cloned into pRS314 (Tang *et al.*, 1997)
pSCD5c-HA-305	DNA fragment encoding Scd5p (79-872 aa) was cloned in frame with a C-terminal *HA* epitope followed by the *ADH1* terminator in pRS305 (Huang *et al.*, 2003)
pEND3n-BD	DNA fragment encoding End3p (1-141 aa) was cloned into pGBKT7
pEND3c-BD	DNA fragment encoding End3p (72-349 aa) was cloned into pGBKT7
pSCD5-N-AD	DNA fragment encoding Scd5p (1-534 aa) was cloned into pGADT7
pSCD5-C-AD	DNA fragment encoding Scd5p (535-872 aa) was cloned into pGADT7
pMyc-END3-314	DNA fragment encoding End3p (1-349 aa) was cloned in frame with an N-terminal *Myc* epitope and placed under its own promoter control in pRS314
pMyc-END3ΔC-314	DNA fragment encoding End3p (1-253 aa) was cloned in frame with an N-terminal *Myc* epitope and placed under its own promoter control in pRS314
pMyc-END3ΔN-314	DNA fragment encoding End3p (116-349 aa) was cloned in frame with an N-terminal *Myc* epitope and placed under its own promoter control in pRS314
pPAN1c-Myc-306	DNA fragment encoding Pan1p (1252-1480 aa) was cloned in frame with a C-terminal *Myc* epitope followed by the *ADH1* terminator in pRS306 (Zeng *et al.*, 2001)
pEND3ΔC-314	DNA fragment encoding End3p (1-253 aa) was placed under its own promoter control in pRS314
pEND3ΔN-314	DNA fragment encoding End3p (116-349 aa) was placed under its own promoter control in pRS314
pGAL-HA-PRK1-316	DNA fragment encoding Prk1p (1-810 aa) was cloned in frame with the *HA* epitope and placed under *GAL1* promoter control in pRS316 (Zeng and Cai, 1999)
pGAL-HA-PRK1^{D158Y}-314	DNA fragment encoding Prk1p (1-810 aa) with D158Y mutation was cloned in frame with the *HA* epitope and placed under *GAL1* promoter control in pRS314 (Zeng and Cai, 1999)
pGEX-LR1	GST-LR1; DNA fragment encoding Pan1p (99-383 aa) was cloned into pGEX-4T-1 (Zeng and Cai, 1999)
pGLC7c-HA-305	DNA fragment encoding Glc7p (60-312 aa) with its upstream 501 base pairs (bp) of the intron was cloned in frame with a C-terminal *HA* epitope followed by the *ADH1* terminator in pRS305
pGLC7^{T152K}c-HA-305	T152K mutation was introduced into pGLC7c-HA-305 by PCR mutagenesis
pPAN1c-Myc-304	DNA fragment encoding Pan1p (1252-1480 aa) was cloned in frame with a C-terminal *Myc* epitope followed by the *ADH1* terminator in pRS304
pGLC7n-td-306	pUb-Arg-DHFR^{ts}-HA-GLC7n-306; The first 200 bp of the *GLC7* open reading frame was generated by PCR and cloned into HindIII site of the plasmid pPW66R (He and Moore, 2005)
pGLC7n-ntd-306	pUb-Arg-DHFR-HA-GLC7n-306; The Leu residue at position 66 in the DHFR moiety (Dohmen *et al.*, 1994) of pUb-Arg-DHFR^{ts}-HA-GLC7n-306 was changed into Pro by PCR mutagenesis
pGEX-SCD5^{WT}	GST-SCD5; DNA fragment encoding Scd5p (409-585 aa) was cloned into pGEX-4T-1 (Huang *et al.*, 2003)
pGEX-SCD5^{AAA}	GST-SCD5 variant with T416A, T450A, T490A mutations (Huang *et al.*, 2003)
pSCD5-HA-316	The *SCD5* gene was generated by PCR and cloned in frame with a C-terminal *HA* epitope followed by the *ADH1* terminator in pRS316
pSCD5$^{PBM2\Delta}$-HA-305	DNA fragment encoding Scd5p (79-872 aa) with mutations on its 2nd PP1-binding motif (KKVRF to AKAAA) was cloned in frame with a C-terminal *HA* epitope followed by the *ADH1* terminator in pRS305
pGLC7^{T152K}c-Myc-305	DNA fragment encoding Glc7p (60-312 aa) with T152K mutation was cloned in frame with a C-terminal *Myc* epitope followed by the *ADH1* terminator in pRS305
pSCD5c-Myc-304	DNA fragment encoding Scd5p (79-872 aa) was cloned in frame with a C-terminal *Myc* epitope followed by the *ADH1* terminator in pRS304
pSCD5^{AAA}-N-BD	DNA fragment encoding Scd5p (1-534 aa) with T416A, T450A, T490A mutations was cloned into pGBKT7
pSCD5^{EEE}-N-BD	DNA fragment encoding Scd5p (1-534 aa) with T416E, T450E, T490E mutations was cloned into pGBKT7
pSCD5^{AAA}-N-AD	DNA fragment encoding Scd5p (1-534 aa) with T416A, T450A, T490A mutations was cloned into pGADT7
pSCD5^{EEE}-N-AD	DNA fragment encoding Scd5p (1-534 aa) with T416E, T450E, T490E mutations was cloned into pGADT7
pGLC7-BD	The *GLC7* coding region was generated by PCR and cloned in frame into pGBKT7
pGAL-PRK1-313	DNA fragment encoding Prk1p (1-810 aa) was generated by PCR and placed under *GAL1* promoter control in pRS313
pPRK1c-GFP-305	DNA fragment encoding PRK1p (439-810 aa) was cloned in frame with a C-terminal *GFP* epitope followed by the *ADH1* terminator in pRS305
pPAN1c-CFP-304	DNA fragment encoding Pan1p (1252-1480 aa) was cloned in frame with a C-terminal *CFP* epitope followed by the *ADH1* terminator in pRS304
pFUR4-424	The *FUR4* gene was generated by PCR and cloned into pRS424
pEND3-424	The *END3* gene was generated by PCR and cloned into pRS424 (Tang *et al.*, 1997)
pSCD5-424	The *SCD5* gene was generated by PCR and cloned into pRS424

oride, 2 mM sodium orthovanadate, 2 mM sodium pyrophosphate, 6 mM β-glycerophosphate) for 2 h before immunoprecipitation was carried out.

Glutathione Transferase (GST) Fusion Proteins and In Vitro Kinase and Phosphatase Assays

To make GST-fusion proteins, DNA fragments were generated by PCR and cloned in-frame into the bacterial GST expression vector pGEX-4T-1 as indicated in Table 2. Expression and purification of GST-fusion proteins followed the published procedure (Zeng and Cai, 1999). Using VIVASPIN 500 columns (Vivascience, Hannover, Germany), GST-fusion proteins were washed and buffer exchanged into either binding buffer (100 mM NaCl, 20 mM HEPES, pH 7.3, 0.1% Triton X-100, and 1 mM dithiothreitol [DTT]) for in vitro binding assay or H_2O for protein phosphatase assay. In vitro kinase assays were performed as described previously (Zeng and Cai, 1999) with slight modifications. The beads-conjugated anti-HA antibody was used to immunoprecipitate HA-Prk1p. GST-fusion proteins were mixed with the immunoprecipitated kinase, 60 μl of HBII buffer, 10 μl of 100 mM ATP, and 10 μl of 250 mM 3-(*N*-morpholino)propanesulfonic acid in a total volume of 200 μl and incubated at 25°C for 3 h, followed by gel electrophoresis and sequential immunoblotting with monoclonal anti-GST (BD Biosciences, Palo Alto, CA) and anti-PThr antibodies. For protein phosphatase assays, yeast extracts containing endogenously expressed Glc7-HA were prepared with phosphatase inhibitor-free lysis buffer (1% Triton X-100, 1% sodium deoxycholate, 0.1% SDS, 50 mM Tris-HCl, pH 7.2, and 1 mM phenylmethylsulfonyl fluoride [PMSF]) supplemented with protease inhibitors (cocktail tablets from Roche Applied Science). Glc7-HA was immunoprecipitated and washed with radioimmunoprecipitation assay buffer (50 mM Tris-HCl, pH 7.2, 150 mM NaCl, 1% Triton X-100, 1% sodium deoxycholate, and 0.1% SDS) five times. The immunoprecipitates, with or without the preincubation with 1 μl of PP1 inhibitor I-2 (New England Biolabs, Ipswich, MA) at 25°C for 15 min, were mixed with phosphorylated GST-fusion proteins and 10 μl of 10× PP1 buffer (New England Biolabs) in a total volume of 100 μl. The mixture was incubated at 37°C, and 20 μl of supernatant was taken at each time point in 20-min intervals. Samples were then subjected to gel electrophoresis and sequential immunoblotting with anti-GST and anti-PThr antibodies.

Two-Hybrid Interaction and In Vitro Binding Assays

For yeast two-hybrid interaction assays, DNA fragments of *SCD5*, *PAN1*, *END3*, and *GLC7* were generated by PCR and cloned into pGBKT7 or pGADT7 vectors as indicated in Table 2. Plasmids were cotransformed into the strain SFY526, and the expression of each fusion protein was confirmed by Western blotting with anti-HA and anti-Myc antibodies. Interactions were quantified by measuring the β-galactosidase activities as instructed by the manufacturer (BD Biosciences). For in vitro binding assays, DNA fragments of *SCD5* were generated by PCR and cloned into pET-32a to fuse with an N-terminal His-epitope. The plasmids were transformed into bacterial strain BL21. Transformants were grown to OD_{600} = 1.0 and incubated with 1 mM isopropylthio-β-d-galactoside at 37°C overnight. Cells were collected by centrifugation and suspended in cold extraction buffer (1% Triton, 150 mM NaCl, 5 mM imidazole, 20 mM Tris-HCl, pH 8.0, and 1 mM PMSF). The suspensions were sonicated on ice, and lysates were centrifuged at 17,000 rpm for 20 min. The supernatants were incubated with prewashed nickel-nitrilotriacetic acid agarose beads (QIAGEN, Valencia, CA) for 1 h at 4°C. After wash with washing buffer (200 mM NaCl, 20 mM HEPES, pH 7.3, 0.1% Triton X-100, and 1 mM DTT) three times, the beads were incubated with GST-fusion proteins in 500 μl of binding buffer for 1 h at 4°C. The bead-bound proteins were washed with washing buffer five times and subjected to gel electrophoresis and sequential immunoblotting with anti-GST and anti-His antibodies.

Actin Staining and Endocytosis Assay

Staining of actin filaments with rhodamine-phalloidin (Invitrogen, Carlsbad, CA) was performed as described previously (Huang *et al*., 2003). The uracil permease internalization assay was carried out according to Volland *et al*. (1994) with minor modifications. Yeast cells were transformed with a multicopy plasmid containing the *FUR4* gene to increase the production of uracil permease. The transformants were grown in uracil dropout medium at 25°C to OD_{600} of 0.2–0.3, and then they were incubated at 37°C for 6 h. Cultures were shifted back to 25°C, and cycloheximide was immediately added to a final concentration of 100 μg/ml. On the addition of cycloheximide, samples were taken at 20-min intervals to assay the uracil permease activity. One milliliter of the culture at each time point was incubated with 5 μl of uracil solution containing 4.5 μl of 1 mM uracil and 0.5 μl of 1 mCi/ml [5,6-^{3}H]uracil (GE Healthcare) for 20 s at 25°C. The mixture was then quickly filtered through a Whatman 25 mm GF/C filter, followed by washing twice with ice-old water and counting for the retained radioactivity.

Live Cell Imaging

Yeast cells expressing GFP and/or cyan fluorescent protein (CFP)-tagged proteins were allowed to grow to early log phase at 30°C. Cells were harvested, resuspended in SC media, and adhered to the surface of a glass slide precoated with 2% agarose. The slide was then covered with a coverslip and sealed with petroleum jelly. Fluorescence microscopy was performed using a Zeiss Axiovert 200 M microscope equipped with a Coolsnap HQ camera (Roper Scientific, Tucson, AZ). All imaging was done by keeping the slide within a closed chamber with a constant temperature of 30°C. Images were acquired continuously at 1 frame/2–5 s, depending on the signal intensity, with motorized GFP and CFP filters. To determine the patch lifetime, >30 patches of each protein were visually analyzed for their time courses between patch appearance and disappearance, and the lifetime was calculated as the average time course ± SD.

RESULTS

Interaction of Scd5p with Pan1p and End3p

To establish the link between Scd5p and Pan1p, we first tested the interaction between the two proteins by yeast two-hybrid assays. As shown in Figure 1A (top right), the N-terminal half of Scd5p displayed a clear interacting activity with the LR2 region of Pan1p. Dissection of SCD5-N into two smaller fragments yielded one with no LR2-binding activity (SCD5-N1) and another with an autoactivity (SCD5-N2). To clarify this issue, we carried out in vitro binding assays using His-tagged Scd5p fragments and GST-LR2. The results showed that SCD5-N2, which contains three Prk1p phosphorylation sites (LxxTxTG), could efficiently pull down GST-LR2 (Figure 1B, lane 6). The interaction between Scd5p and Pan1p was further confirmed by coimmunoprecipitation. Endogenously expressed Scd5-HA could be pulled down by the anti-Myc antibody when Pan1-Myc was coexpressed (Figure 1C, lane 4), indicating that Scd5p interacts with Pan1p in vivo.

Concurrently, we also tested the possibility of an interaction between Scd5p and End3p, which is known to form a complex with Pan1p in vivo (Tang *et al*., 1997). Two-hybrid assays revealed that SCD5-N could bind to the N terminus of End3p (Figure 1A, bottom right), which is noteworthily not involved in the interaction with Pan1p (Tang *et al*., 1997). This result was again supported by coimmunoprecipitation experiments (Figure 1D). We could not, however, detect an interaction between Scd5p and Sla1p, another endocytic protein that associates with Pan1p and End3p in vivo (Tang *et al*., 2000), by the two-hybrid assay (data not shown). In support of the finding that Scd5p interacts with both Pan1p and End3p, a temperature-sensitive mutant of *scd5* defective in endocytosis and actin organization, *scd5-1* (Chang *et al*., 2002; Huang *et al*., 2003), exhibited synthetic lethality with either *pan1-4* (Tang and Cai, 1996), or *end3*Δ (Figure 1E), indicating that these genes have functions in common. Together, these experiments confirm a physical and functional association between Scd5p and the Pan1p–End3p complex, thus making Scd5p a possible link between Glc7p and Pan1p for the dephosphorylation purpose.

Elevation of Pan1p Phosphorylation Level in scd5 and end3 Mutants

Pan1p is known to be phosphorylated by Prk1p on potentially a large number of threonine residues present as the LxxQxTG motifs and clustered in the LR1 and LR2 regions (Zeng and Cai, 1999). The steady-state phosphorylation level of endogenously expressed Pan1p could be revealed by a phosphothreonine-specific antibody (anti-PThr), as shown in Figure 2A (left, lane 2). As expected, it was drastically reduced in the *prk1*Δ mutant (to ~15% of the wild-type control). In contrast, the Pan1p phosphorylation level was found to be significantly increased in the *scd5-1* mutant at the nonpermissive temperature of 37°C (Figure 2B). This result shows that the phosphorylation status of Pan1p in vivo is dependent on the activity of Scd5p. As the *scd5-1* allele is impaired in binding to Glc7p (Chang *et al*., 2002;

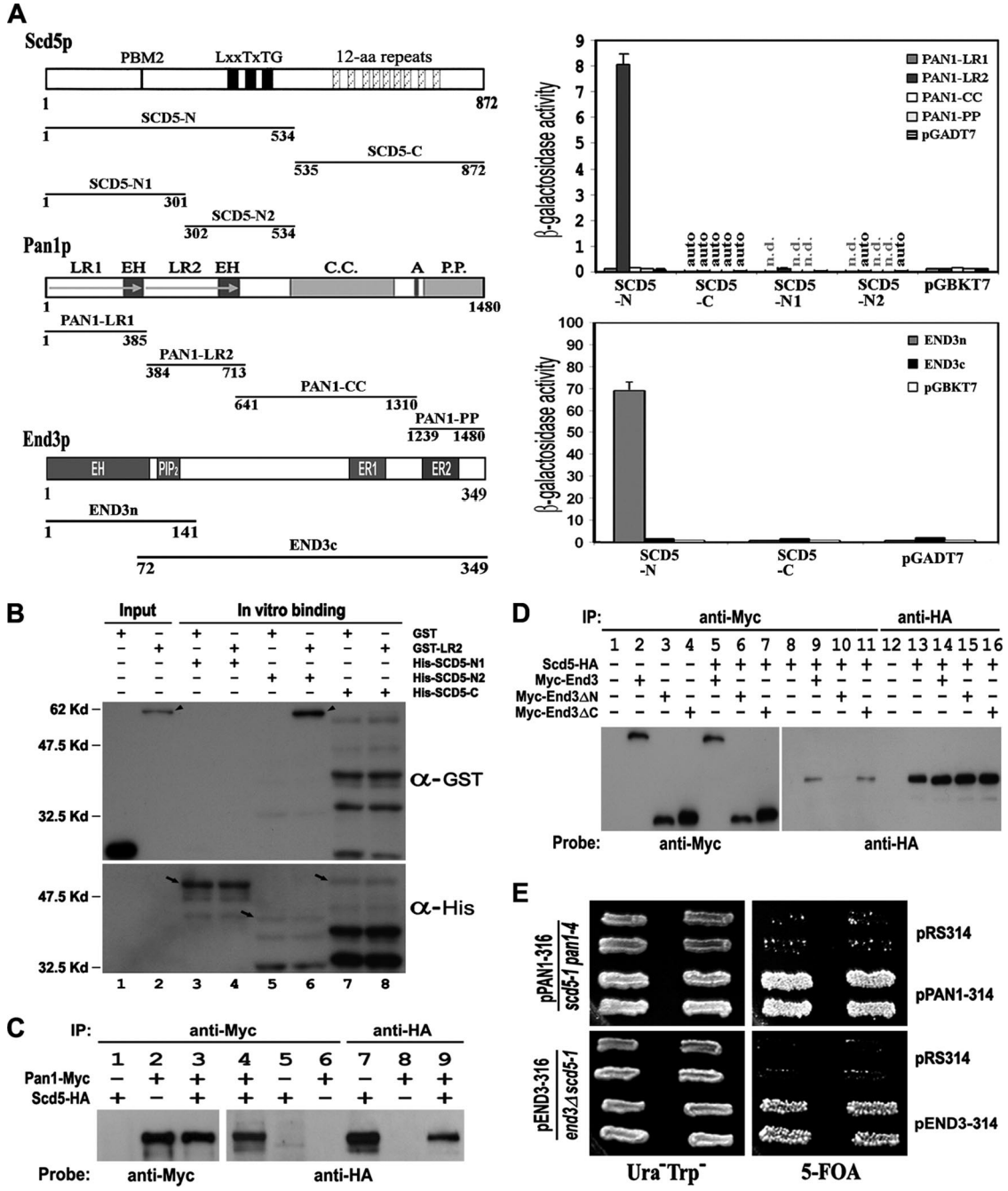

Figure 1. Interactions of Scd5p with Pan1p and End3p. (A) Two-hybrid interactions of Scd5p with Pan1p and End3p. The regions of Scd5p, Pan1p, and End3p used for two-hybrid assays were schematically shown on left. Domains and motifs important for each protein are also indicated. PBM, phosphatase binding motif; LR, long repeat; EH, Eps15 homology; C.C., coiled-coil; A, acidic motif; P.P., polyproline; PIP_2, phosphatidylinositol 4,5-bisphosphate binding motif; ER, End3 repeat. Two-hybrid interactions were quantified by measuring β-galactosidase activity and expressed in Miller units with SD. Results are the average of three independent transformants. auto, autoactivity; n.d., not determined. (B) In vitro binding assays between Scd5p and Pan1p. Different fragments of His-tagged Scd5p (arrows) were bead immobilized and incubated with GST-LR2 (arrowhead) or GST, respectively. The precipitates, as well as portions of GST and GST-LR2 (loaded on lanes 1–2 as positive controls), were separated by gel electrophoresis and sequentially immunoblotted with anti-GST and anti-His antibodies. A cross-reaction between anti-GST antibody and His-SCD5-C was observed (lanes 7 and 8). (C) Coimmunoprecipitation of Scd5p with Pan1p. Yeast extracts prepared from YMC448 (lanes 1, 5, and 7), YMC441 (lanes 2, 6, and 8), or YMC471 (lanes 3–4 and 9), were subjected to anti-Myc or anti-HA immunoprecipitation followed by gel electrophoresis, and then they were immunoblotted with anti-Myc and anti-HA antibodies, as indicated. (D) Coimmunoprecipitation of Scd5p with End3p. Yeast extracts prepared from YMC448 (lanes 8 and 13), YMC474 containing pMyc-End3-314 (lane 2), YMC474 containing pMyc-End3ΔN-314 (lane 3), YMC474 containing pMyc-End3ΔC-314 (lane 4), YMC476 containing pMyc-End3-314 (lanes 5, 9, and 14), YMC476 containing pMyc-End3ΔN-314 (lanes 6, 10, and 15), and YMC476 containing pMyc-End3ΔC-314 (lanes 7, 11, and 16), were subjected to anti-Myc or anti-HA immunoprecipitation followed by gel electrophoresis, and immunoblotted with anti-Myc and anti-HA antibodies, as indicated. (E) Genetic interactions of Scd5p with Pan1p and End3p. YMC472 transformed with pRS314 or pPAN1-314 (top) and YMC475 transformed with pRS314 or pEND3–314 (bottom) were tested for growth on synthetic complete medium containing 1 mg/ml 5-fluoroorotic acid at 25°C for 5 d.

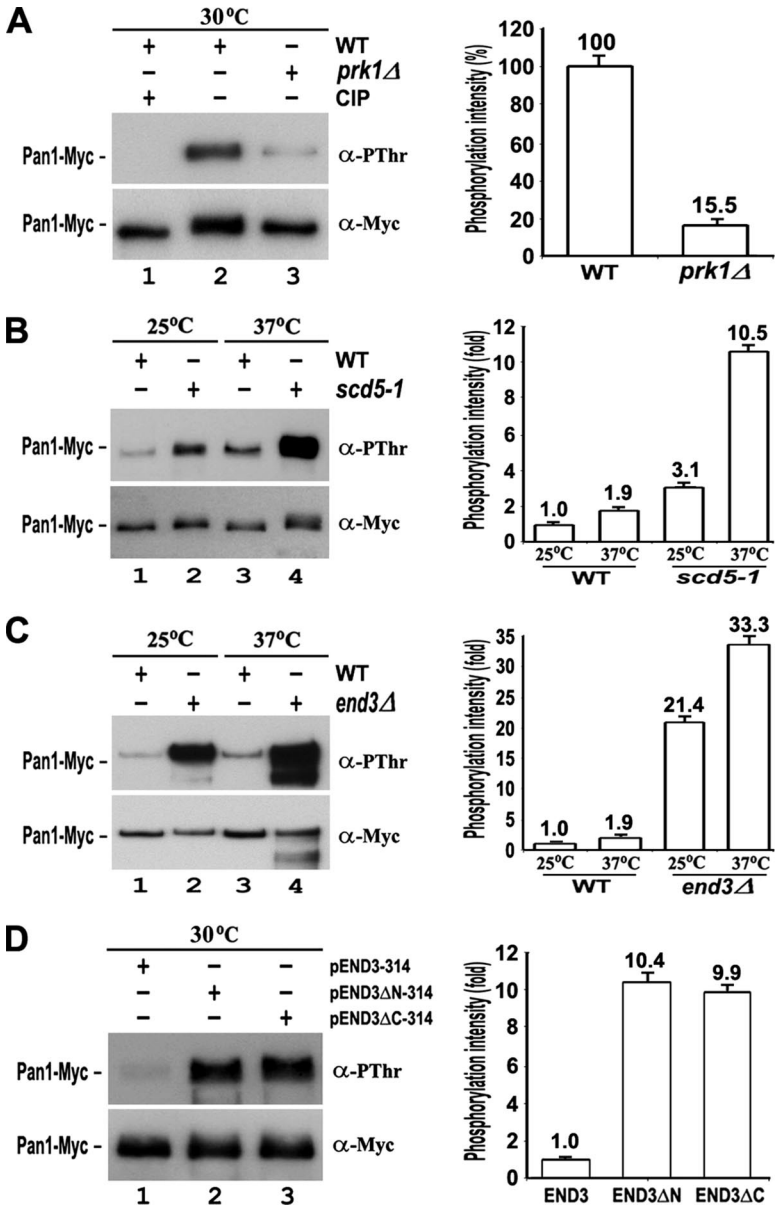

Figure 2. Phosphorylation level of Pan1p in *scd5* and *end3* mutants. Endogenously expressed Pan1-Myc was immunoprecipitated from cells and sequentially immunoblotted with anti-PThr and anti-Myc antibodies. (A) Pan1-Myc from YMC441 (lanes 1 and 2) and YMC478 (lane 3) cells at 30°C. The immunoprecipitates in lane 1 were incubated with 1 μl of CIP for 30 min at 37°C before loading. (B) Pan1-Myc from YMC441 (lanes 1 and 3) and YMC479 (lanes 2 and 4) cells at either 25°C (lanes 1 and 2) or 37°C for 3 h (lanes 3 and 4). (C) Pan1-Myc from YMC441 (lanes 1 and 3) and YMC480 (lanes 2 and 4) cells at either 25°C (lanes 1 and 2) or 37°C for 3 h (lanes 3 and 4). (D) Pan1-Myc from YMC480 cells containing pEND3–314 (lane 1), pEND3ΔN-314 (lane 2), or pEND3ΔC-314 (lane 3) at 30°C. The phosphorylation level of Pan1-Myc in each sample was measured by densitometer (GS800; Bio-Rad, Hercules, CA) and normalized against its protein amount. The relative phosphorylation intensities were calculated and presented as bar graphs (right).

Huang *et al*., 2003), the elevation of Pan1p phosphorylation level in this mutant is likely resulted from a deficient access of Glc7p to Pan1p.

End3p may also have a crucial role in Pan1p dephosphorylation, because it has a stronger Scd5p-interacting activity than Pan1p in two-hybrid assays (Figure 1A). More importantly, the interaction between End3p and Pan1p has recently been found to be unaffected by the presence of the Prk1 kinase (Toshima *et al*., 2007). This is consistent with our domain mapping data showing the region of Pan1p involved in binding with End3p to be located immediately after the second EH domain, and hence outside of the Prk1 phosphorylation region (data not shown). End3p, therefore, could be a preferred entry point for Scd5p-Glc7p to gain access to phosphorylated Pan1p. The level of Pan1p phosphorylation in the *end3*Δ mutant was indeed markedly elevated (Figure 2C). However, it remained unclear whether this was due to a loss of access for Scd5p-Glc7p, or an overphosphorylation by Prk1p, as the binding of End3p could help shield Pan1p from Prk1p phosphorylation (Zeng and Cai, 1999), or both. To answer this question, we examined different truncation mutants of *end3*. End3p interacts with Scd5p and Pan1p through its N- and C-terminal regions respectively, and removal of either will disable its function as a bridging agent between Scd5p and Pan1p, resulting in an increase in the level of Pan1p phosphorylation. This was indeed the case (Figure 2D). Both End3ΔN and End3ΔC mutant proteins complemented the temperature sensitivity of the *end3* null mutant (data not shown), as reported previously (Benedetti *et al*., 1994), indicating that they were expressed functionally in the cells. Since the C-terminal region of End3p was still capable of binding Pan1p (Tang *et al*., 1997), the role of End3p is probably more in promoting Pan1p dephosphorylation than protecting it from phosphorylation.

Dephosphorylation of Pan1p by Glc7p In Vitro and In Vivo

Next, we sought to test whether Glc7p could directly dephosphorylate Pan1p in vitro. To obtain the phosphorylated

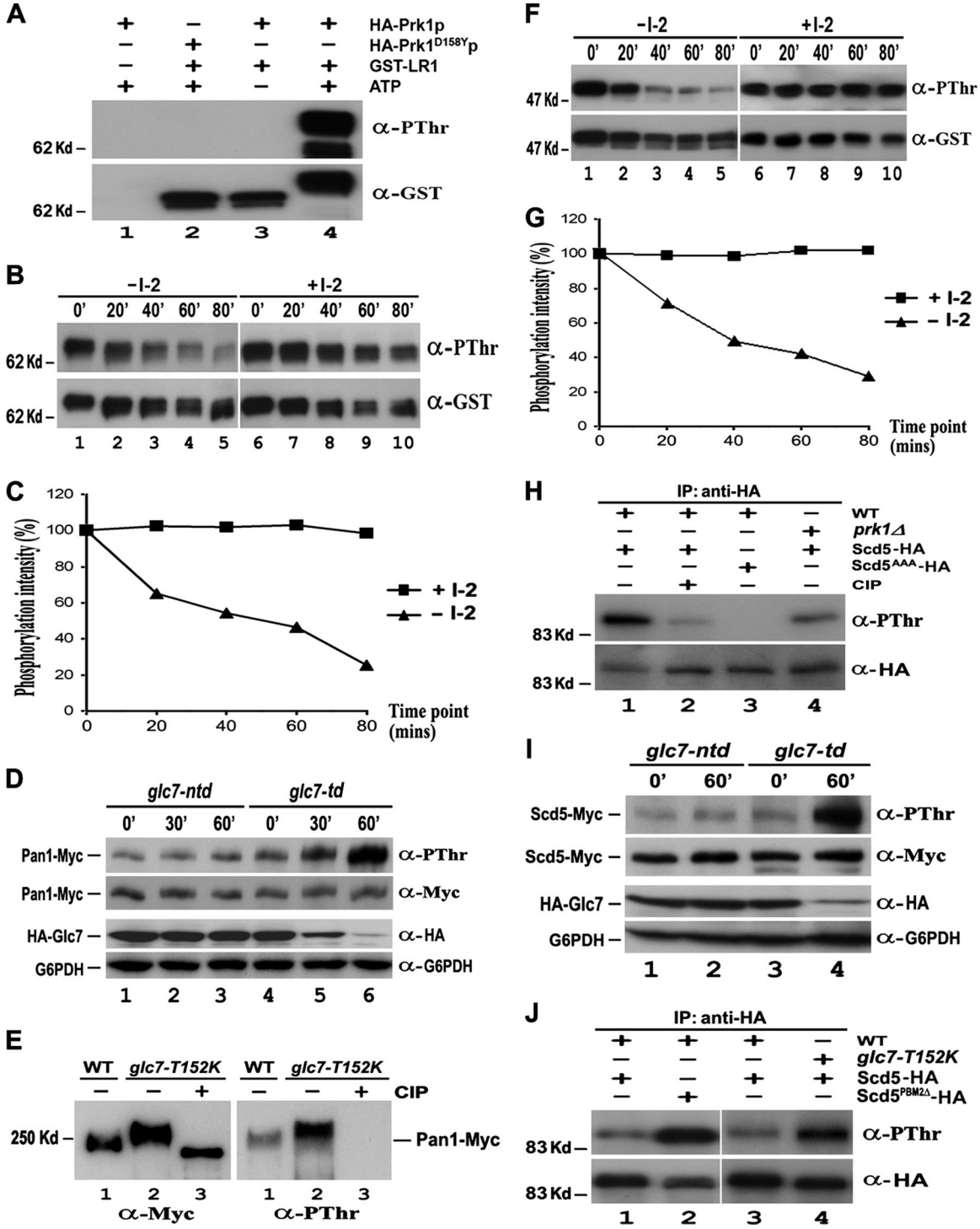

Figure 3. Dephosphorylation of Pan1p and Scd5p by Glc7p in vitro and in vivo. (A) In vitro phosphorylation of Pan1p by Prk1p. Purified GST-LR1 was incubated with immunoprecipitated HA-Prk1p (lanes 3 and 4) or HA-Prk1^{D158Y}p (lane 2) in the presence (lanes 2 and 4) or absence (lane 3) of nonradioactive ATP at 25°C for 3 h. The mixture was separated by gel electrophoresis and immunoblotted with anti-PThr and then anti-GST antibodies. (B and F) In vitro dephosphorylation of Pan1p (B) and Scd5p (F) by Glc7p. Immunoprecipitated Glc7-HA with or without the I-2 treatment was incubated with in vitro phosphorylated GST-LR1 or GST-SCD5 at 37°C. Samples were taken at 20-min intervals, electrophoresed, and immunoblotted with anti-PThr and anti-GST antibodies. (C and G) Measurement of Glc7p phosphatase activity on Pan1p (C) and Scd5p (G). The phosphorylation level of GST-LR1 (Figure 3B) and GST-SCD5 (Figure 3F) at each time point was measured by densitometer and normalized against its protein amount. (D) Pan1p phosphorylation level in *glc7-td* mutant. YMC484 (lanes 4–6) and YMC485 (lanes 1–3) cells were allowed to grow to the log phase at 25°C and then shifted to 37°C. Samples were taken at 0, 30, and 60 min, and Pan1p-Myc was immunoprecipitated, electrophoresed, and immunoblotted with anti-PThr and then anti-Myc antibodies. Total proteins of each sample also were extracted by TCA precipitation and subjected to Western analysis to assay the expression level of Glc7p. (E) Pan1p phosphorylation level in *glc7-T152K* mutant. Pan1-Myc was immunoprecipitated from YMC441 (lane 1) and YMC482 (lanes 2–3) cells grown at 30°C. The immunoprecipitates in lane 3 were preincubated with CIP for 30 min before loading. (H) Phosphorylation of Scd5p

form of Pan1p, GST-LR1, which contains multiple Prk1p phosphorylation sites (Zeng and Cai, 1999), was subjected to phosphorylation by Prk1p in the presence of nonradioactive ATP. As shown in Figure 3A, GST-LR1 could be detected by the anti-PThr antibody after an incubation with immunoprecipitated HA-Prk1p, and no signal was detected if a kinase-dead mutant, Prk1^{D158Y}p (Zeng and Cai, 1999), was used. The phosphorylated GST-LR1 thus obtained gradually reduced its phosphorylation level during incubation with immunoprecipitated Glc7-HA to, for example, ~20% after 80 min (Figure 3, B and C). This reduction in GST-LR1 phosphorylation was effectively blocked by I-2 (Figure 3, B and C), a phosphatase inhibitor previously demonstrated to be specific for type 1 protein phosphatases (Cohen *et al*., 1989). Similar results were also obtained using phosphorylated GST-LR2 as the substrate in the assay (data not shown). These experiments confirmed that Glc7p could execute dephosphorylation of Pan1p in vitro.

We further examined the effect of Glc7p on the phosphorylation level of Pan1p in vivo. To create a conditional mutant of Glc7p, a *GLC7* construct containing a heat-inducible degradation signal fused to the N terminus (He and Moore, 2005), along with an HA epitope, was obtained and used to replace the wild type locus in our test strain. The mutant thus created, *glc7-td*, displayed a temperature-dependent decline in the amount of Glc7p protein (Figure 3D). The depletion of Glc7p was not observed if the degradation signal in the mutant was disrupted (Figure 3D, *glc7-ntd*). It is evident that the phosphorylation level of Pan1p in *glc7-td* cells increased in accordance with the depletion of Glc7p, while remained unchanged if Glc7p was not degraded (Figure 3D and Supplemental Figure S1A). Moreover, another mutant, *glc7-T152K*, previously characterized to be defective in association with Scd5p (Tu *et al*., 1996), also exhibited an elevated level of Pan1p phosphorylation (Figure 3E and Supplemental Figure S1B). These results allowed us to conclude that Glc7p, through its binding to Scd5p, is required for dephosphorylation of Pan1p in vivo.

Dephosphorylation of Scd5p by Glc7p In Vitro and In Vivo

Similar to Pan1p, Scd5p is also phosphorylated by Prk1p, and the phosphorylation sites are adjacent to the Glc7p binding motif (Henry *et al*., 2003; Huang *et al*., 2003). Therefore, Scd5p may also undergo dephosphorylation by Glc7p. To evaluate the effect of Glc7p on the phosphorylation status of Scd5p, we applied the similar assays as described above to Scd5p. First, purified GST-SCD5 was made suitable for in vitro phosphatase assay by incubation with nonradioactive ATP and Prk1p, and the resultant phosphorylated GST-SCD5 was assayed with immunoprecipitated Glc7-HA. As shown in Figure 3, Glc7p could efficiently dephosphorylate GST-SCD5 in vitro, and again, a preincubation with I-2 completely inhibited the Glc7p activity (Figure 3, F and G). Next, the phosphorylation status of Scd5p in vivo was analyzed. The steady-state phosphorylation level of Scd5p in wild-type cells turned out to be below detection, owing likely to the complex formation with Glc7p in vivo (Chang *et al*., 2002). It was possible to increase the basal phosphorylation level of Scd5p by adding phosphatase inhibitors to the culture medium (Figure 3H). Deletion of *PRK1* reduced Scd5p phosphorylation to 36% of the wild-type level under the same condition, whereas disruption of Prk1p phosphorylation sites (SCD5^{AAA}) extinguished the signal (Figure 3H and Supplemental S1C), indicating that Scd5p was phosphorylated mainly by Prk1p, although other Prk1p-like kinases (Ark1p or Akl1p) could also phosphorylate Scd5p in the absence of Prk1p (Henry *et al*., 2003). Similarly to Pan1p, the level of phosphorylated Scd5p was substantially increased in the *glc7-td* mutant after the phosphatase was depleted by temperature shift (Figure 3I and Supplemental Figure S1D). Moreover, the increase in the Scd5p phosphorylation level was also observed in cells containing either the T152K mutation on Glc7p or PBM2Δ on Scd5p (Figure 3J and Supplemntal S1E), both of which are known to impair the interaction between Glc7p and Scd5p (Tu *et al*., 1996; Chang *et al*., 2002; Huang *et al*., 2003). These results demonstrated that the activity of Glc7p and its interaction with Scd5p are required for maintaining Scd5p in an un- or underphosphorylated state in vivo.

Partial Suppression of glc7-td by prk1Δ

The involvement of Glc7p in dephosphorylation of Pan1p and Scd5p in vivo suggests that it plays an antagonistic role to the Prk1p kinase in the regulation of actin and endocytosis. To investigate the functional relationship between the phosphatase and the kinase, we examined the actin cytoskeleton organization in the respective mutants. As shown in Figure 4A, the *glc7-td* mutant exhibited a grossly distorted actin cytoskeleton after a prolonged incubation at 37°C (6 h) to diminish the Glc7p protein content (Figure 4A, center). The majority of *glc7-td* cells contained large and aberrant actin aggregates similar to those found in the *pan1-4*, *scd5-1*, and *end3*Δ mutants (Benedetti *et al*., 1994; Tang and Cai, 1996; Huang *et al*., 2003). In contrast, the control cells (*glc7-ntd*) maintained a normal pattern of actin cytoskeleton after the same treatment (Figure 4A, top), suggesting that the actin abnormalities in *glc7-td* cells were caused by the phosphatase depletion. Remarkably, the actin defects in *glc7-td* cells could be largely reversed by deletion of *PRK1*, because the *prk1*Δ *glc7-td* cells generally showed normal-looking cortical patches, although some aberrant actin aggregates were still visible in a minority of the double mutant cells (Figure 4A, bottom). This result is consistent with the proposed functional antagonism between Glc7p and Prk1p in the regulation of actin cytoskeleton organization.

To see whether depletion of Glc7p also results in an endocytic defect, we carried out the uracil permease internalization assay, by which the endocytic defect could be measured quantitatively. The yeast uracil permease is a plasma membrane protein that is internalized for degradation via the endocytic pathway (Volland *et al*., 1994). As shown in Figure 4B, after 6 h of incubation at 37°C, the control cells of *glc7-ntd* internalized uracil permease normally and exhibited a rapid decrease in uracil uptake upon addition of

Figure 3 (cont). in vivo. YMC448 (lanes 1–2), YMC449 (lane 3), and YMC488 (lane 4) cells expressing either Scd5-HA (lanes 1 and 2 and 4) or Scd5^{AAA}-HA (lane 3) were grown at 30°C and incubated with phosphatase inhibitor cocktail for 2 h. The HA-tagged proteins were immunoprecipitated, electrophoresed, immunoblotted with anti-PThr and then anti-HA antibodies. (I) Scd5p phosphorylation level in *glc7-td* mutant. Log phase YMC492 (lanes 1 and 2) and YMC493 (lanes 3 and 4) cells at 25°C were incubated with phosphatase inhibitor cocktail for 2 h and shifted to 37°C. Samples were taken at 0 and 60 min, and Scd5-Myc was immunoprecipitated, electrophoresed, and immunoblotted with anti-PThr and then anti-Myc antibodies. The expression level of Glc7p in each time point was also assayed by Western analysis. (J) Scd5p phosphorylation level in cells containing either T152K mutation on Glc7p or PBM2Δ mutation on Scd5p. Log phase YMC487 (lanes 1 and 3), YMC490 (lane 4), and YMC489 (lane 2) cells at 25°C were shifted to 37°C for 4 h with phosphatase inhibitor cocktail present during the last 2 h. The HA-tagged proteins were immunoprecipitated, electrophoresed, and immunoblotted with anti-PThr and then anti-HA antibodies.

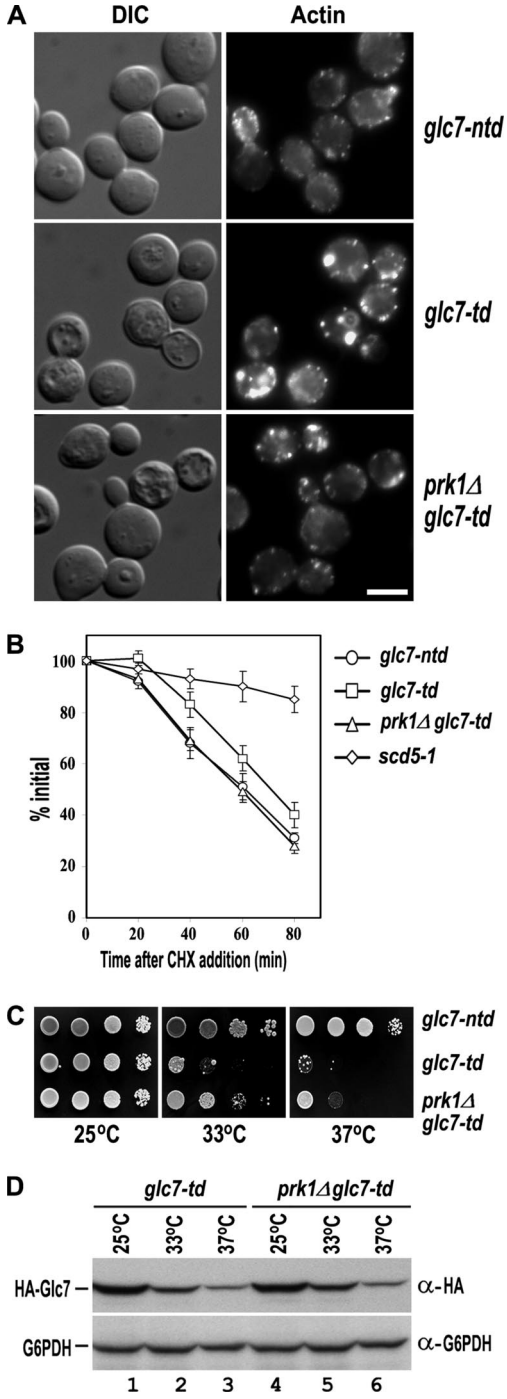

Figure 4. Suppression of *glc7-td* by *prk1*Δ. (A) Actin staining of *glc7-ntd* (YMC499), *glc7-td* (YMC500), and *prk1*Δ *glc7-td* (YMC501) cells. The strains were grown at 25°C to early log phase and incubated at 37°C for 6 h followed by fixation and staining with rhodamine-phalloidin. Bar, 4 μm. (B) Uracil permease internalization assay of *glc7-ntd*, *glc7-td*, *prk1*Δ *glc7-td*, and *scd5-1* cells. The cells were transformed with pFUR4-424, and the transformants were grown at 25°C to OD_{600} of 0.2–0.3. After incubated at 37°C for 6 h, cultures were brought back to 25°C, and the internalization of uracil permease was initiated by the addition of cycloheximide (CHX). Transport of [^{3}H]uracil into yeast cells was used as a measurement for the relative amount of uracil permease retained on the cell surface. Uracil uptake is plotted as the percentage activity relative to the initial time point. The results shown are the averages of two independent assays. (C) The growth of *glc7-ntd*, *glc7-td*, and *prk1*Δ glc7-td strains at different temperatures. Cells were grown at 25°C to OD_{600} of 0.5, and 10× serial dilutions of each culture were dropped onto $CuSO_4$-containing plates for incubation at the indicated temperatures for 2 d. (D) Comparison of the Glc7p protein level in *glc7-td*, and *prk1*Δ *glc7-td* strains. Cells were grown at 25°C to log phase and then shifted to either 33°C or 37°C for 1 h. Samples were taken at 0 and 60 min. Total proteins of each sample were prepared and subjected to Western analysis.

cycloheximide to suppress protein synthesis. In contrast, the *scd5-1* cells, whose severe endocytic defects had been reported before (Huang *et al.*, 2003), maintained a high activity of uracil uptake. Under the same condition, the *glc7-td* cells showed a mildly but consistently slower decline in uracil uptake activity, indicating that the internalization of uracil permease was somewhat impaired in these cells (Figure 4B). The mild retardation in the loss of uracil uptake activity of the *glc7-td* cells was clearly attributable to the diminished phosphatase activity, because it could be corrected by removal of the Prk1p kinase. The *prk1*Δ *glc7-td* double mutant cells internalized uracil permease as efficiently as *glc7-ntd* cells (Figure 4B). The mild rather than severe defect in endocytosis in the *glc7-td* cells, as opposed to the actin defects described above, is likely due to the fact that the depletion of the phosphatase under these conditions was hardly complete, and the residual amount of Glc7p remained detectable even after 6 h of incubation at 37°C (data not shown). These observations suggest that the aspect of function of the Pan1p-associated complex with respect to actin is more sensitive to the Prk1p phosphorylation than that with respect to endocytosis.

Furthermore, we found that the growth defect of *glc7-td* mutant could also be partially suppressed by *prk1*Δ. As shown in Figure 4C, the *glc7-td* cells grew well at 25°C but could not sustain the growth at either 33 or 37°C. Deletion of the *PRK1* gene rendered the *glc7-td* cells capable of much better growth at these temperatures, even though they were eventually still inviable (Figure 4C). This partial suppression of *glc7-td* by *prk1*Δ was not due to any recovery of the Glc7p protein level, because the level of the phosphatase remained same in both *glc7-td* and *prk1*Δ *glc7-td* cells at 25°C, and it was diminished at a similar rate at 33 and 37°C (Figure 4D).

Regulation of Scd5p-dependent Interactions by Prk1p Phosphorylation

To gain more insight into the mechanism of dephosphorylation of Pan1p by Glc7p, we examined the interactions among Scd5p, Pan1p, End3p, and Glc7p in more detail. The conspicuously low in vivo phosphorylation level of Scd5p led us to consider the prospect that Scd5p must be present in an unphosphorylated form to fulfill its role as a phosphatase-targeting factor. It is worth noting that both Pan1p and End3p bind to the region of Scd5p where the three Prk1p phosphorylation sites are located (Figure 1). Prk1p phosphorylation has been shown to disfavor the multivalent interaction between Pan1p and other proteins (Zeng *et al.*, 2001; Toshima *et al.*, 2005). It is therefore important to find out whether the interactions of Scd5p with Pan1p, End3p, and Glc7p could be affected by Prk1p phosphorylation on Scd5p. Mutations were generated at the Prk1p phosphorylation sites of Scd5p to convert the three T residues into either A or E to mimic unphosphorylated and phosphorylated states of Scd5p, respectively. Two-hybrid assays revealed that these mutations affected the interactions of Scd5p with both Pan1p and End3p, but not with Glc7p (Figure 5, A–C). Compared with the wild-type, Scd5^{AAA}p

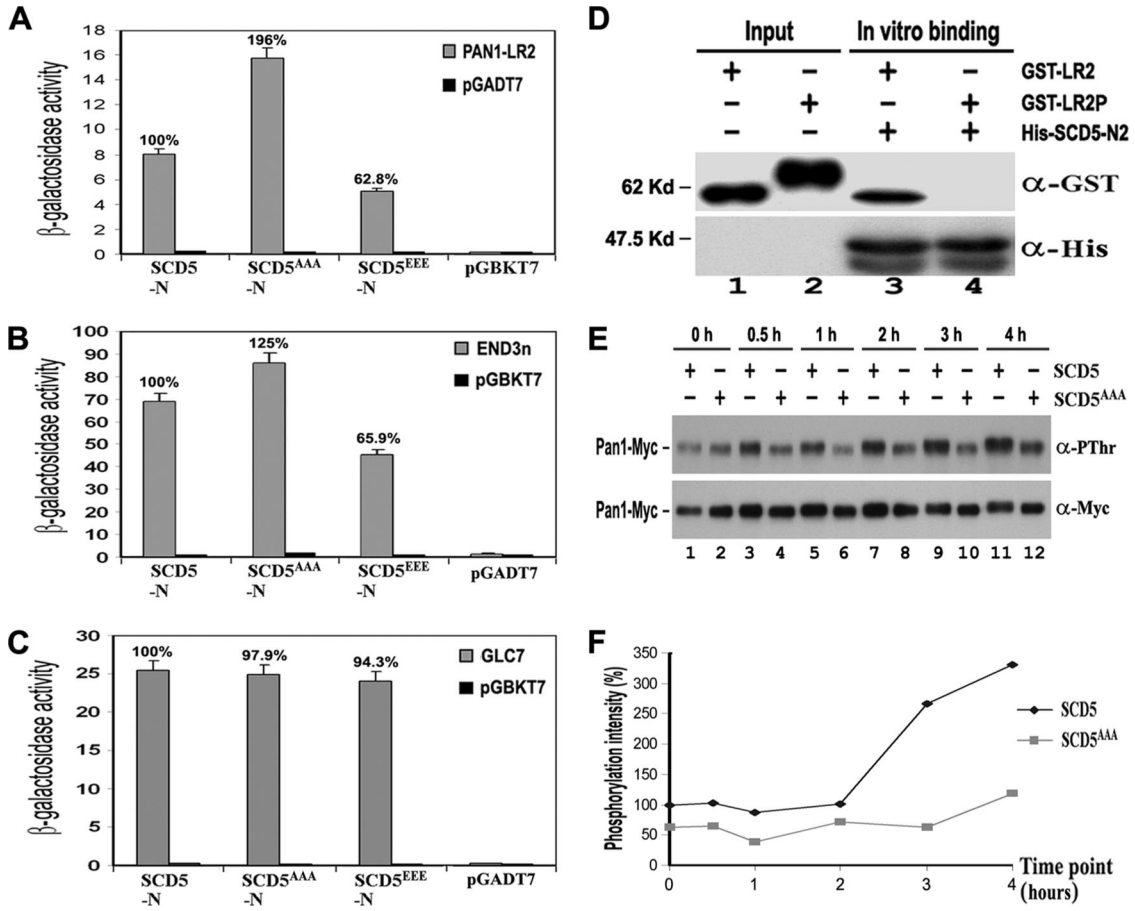

Figure 5. Phosphoregulation of Scd5p-related interactions. (A–C) Two-hybrid interactions of wild-type (SCD5), SCD5^{AAA}, and SCD5^{EEE} with Pan1p (A), End3p (B), and Glc7p (C). (D) In vitro binding assays between Scd5p and phosphorylated Pan1p. His-tagged SCD5-N2 was immobilized and incubated with unphosphorylated GST-LR2 (lane 3) and phosphorylated GST-LR2P (lane 4), respectively. The precipitates, together with portions of GST-LR2 and GST-LR2P (lanes 1–2), were separated by gel electrophoresis and sequentially immunoblotted with anti-GST and anti-His antibodies. (E) The effect of SCD5^{AAA} mutation on Prk1p-induced Pan1p phosphorylation. YMC471 and YMC473 cells containing pGAL-PRK1-313 were allowed to grow at 30°C to log phase in raffinose, followed by addition of galactose. Samples were taken at the indicated time points. Pan1-Myc was immunoprecipitated, electrophoresed, and immunoblotted with anti-PThr and anti-Myc antibodies. (F) Calculation of the relative phosphorylation intensity of Pan1-Myc in Figure 5E. The phosphorylation level of Pan1-Myc in each lane was measured by densitometer and normalized against its protein amount. The relative phosphorylation intensities of all lanes were calculated against lane 1.

exhibited a stronger binding activity with both Pan1p and End3p (increased to 196% for Pan1p and 125% for End3p), whereas Scd5^{EEE}p showed a considerably reduced binding, to ~60%, with the two proteins (Figure 5, A and B). These results are of a good indication that the interactions of Scd5p with Pan1p and End3p are both negatively regulated by phosphorylation on Scd5p. The binding with phosphatase Glc7p, in contrast, remained at a similar level irrespective of mutations (Figure 5C), suggesting that the Scd5p–Glc7p interaction was not affected by Scd5p phosphorylation. We also examined the effect of Pan1p phosphorylation on its interaction with Scd5p using an in vitro binding assay. As shown in Figure 5D, the bead-bound His-SCD5-N2 was able to bind unphosphorylated GST-LR2 efficiently, but failed to do the same to phosphorylated GST-LR2. These results suggest that Scd5p may not be able to target Glc7p to the phosphorylated Pan1p directly. Instead, it may do so via its binding to End3p, whose association with Pan1p in vivo is not affected by phosphorylation of Pan1p (Toshima *et al.*, 2007).

The observation that phosphorylation of Scd5p impairs its interaction with the Pan1p–End3p complex suggests that the dissociation of Scd5p from Pan1p-End3p is one of the consequences after Prk1p phosphorylation. If this is the case, it will be interesting to find out whether the phosphorylation and dissociation of Scd5p is required for, or independent of, the phosphorylation of Pan1p. To address this question, we overexpressed the *PRK1* gene from the *GAL1* promoter to enhance the Pan1p phosphorylation in vivo in the nonphosphorylatable *scd5^{AAA}* mutant. As shown in Figure 5, E and F, the level of Pan1p phosphorylation in the wild-type cells was elevated ~3.5-fold after 4 h of kinase overexpression. In contrast, the *scd5^{AAA}* mutant, whose steady-state Pan1p phosphorylation level was already lower before the induction, only showed a slight increase under the same conditions (Figure 5, E and F). This result suggests that phosphorylation of Pan1p has to be preceded by the phosphorylation of Scd5p in vivo. Scd5p, therefore, may serve as a switch in the event of Pan1p phosphorylation in addition to its role as a phosphatase-targeting factor.

Live Cell Imaging of Pan1p, Scd5p, and Prk1p

To correlate the above-mentioned studies with the patterns of protein localization, we examined the real-time protein

dynamics of Pan1p, Scd5p, and Prk1p in live cells. In agreement with previous studies (Kaksonen *et al*., 2003, 2005; Sun *et al*., 2006), the Pan1-GFP–labeled cortical patches showed restricted movement and exhibited a patch lifetime of ~28 s (Figure 6, A and B, and Supplemental Movie 1). The Scd5-GFP patches were virtually of the same pattern of dynamics with a life span of ~27 s (Figure 6, A and B, and Supplemental Movie 2). The Prk1-GFP patches, on the other hand, had a shorter lifetime (~17 s) and higher motility (Figure 6, A and B, and Supplemental Movie 3). Two-color imaging revealed that Scd5-GFP was recruited to cortical patches at the same point as Pan1-CFP, and the two proteins colocalized with each other on most of the patches, and disappeared together in the end (Figure 6, C–E, and Supplemental Movie 4). In contrast, Prk1-GFP joined the Pan1-CFP patches at a much later stage, just a few seconds before Pan1-CFP began to fade. It coexisted with Pan1-CFP transiently, and vanished shortly after the disappearance of Pan1-CFP (Figure 6, F–H, and Supplemental Movie 5). These data support the earlier suggestion that the Pan1p and Scd5p are components of the same endocytic complex, and phosphorylation by Prk1p leads to their dissociation. The disappearance of Pan1p and Scd5p from cortical patches shortly after the

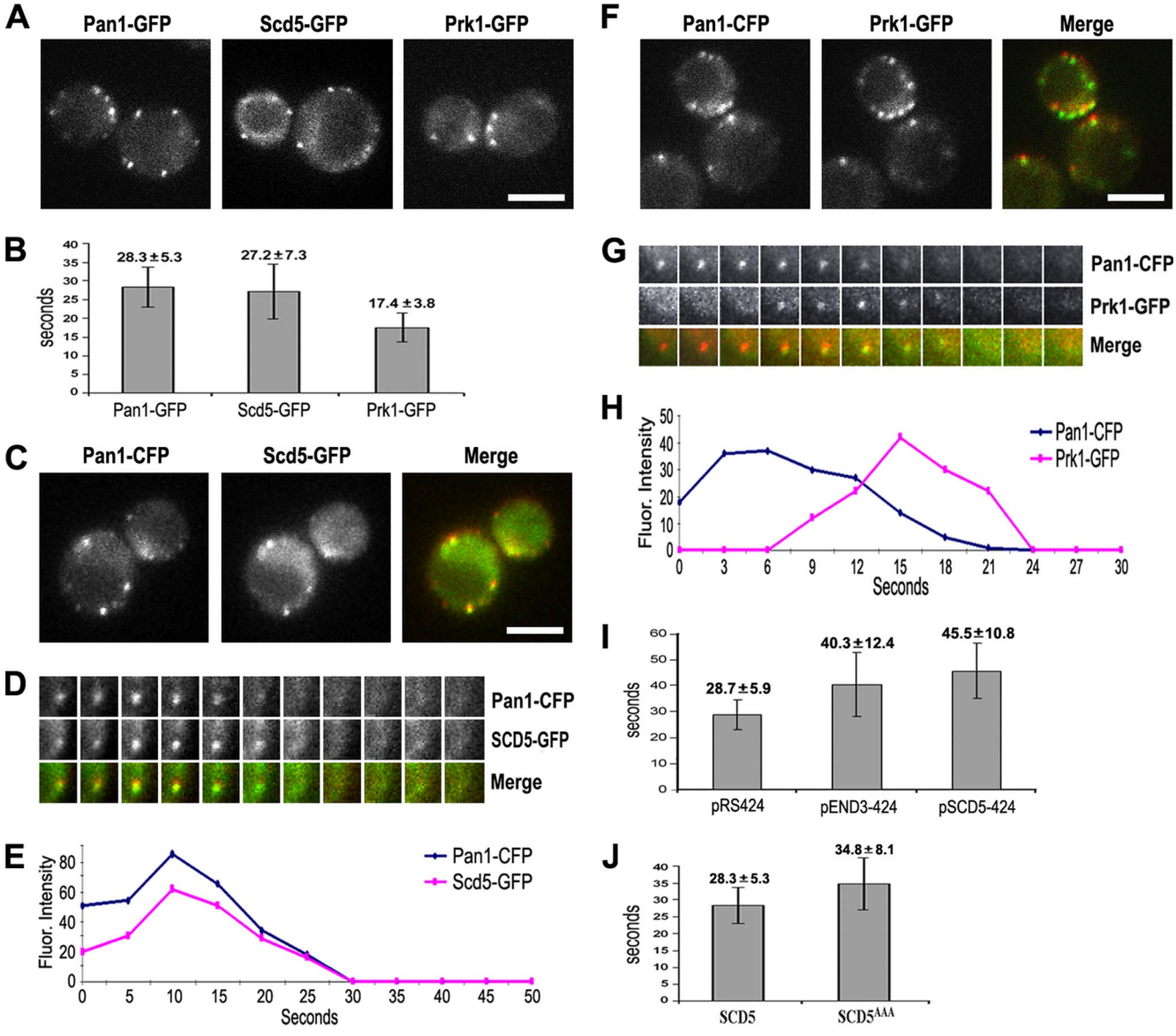

Figure 6. Live cell imaging of Pan1p, Scd5p, and Prk1p patches. (A) Single frames from movies of wild-type cells expressing Pan1-GFP (YMC494), Scd5-GFP (YMC496), and Prk1-GFP (YMC495). Movies were taken with the frame intervals of 2 s for Pan1-GFP and Prk1-GFP, and 4 s for Scd5-GFP. See Supplemental Movies S1–S3. (B) Lifetimes ± SD of Pan1-GFP, Scd5-GFP, and Prk1-GFP patches in wild-type cells. $n \geq 30$ for each protein. (C and F) Single frames from two-color movies of live cells expressing Pan1-CFP and Scd5-GFP (YMC498; C) or Pan1-CFP and Prk1-GFP (YMC497; F). Movies were taken with frame intervals of 5 s for C and 3 s for F. See Supplemental Movies S4 and S5. (D and G) Time series from two-color movies showing the dynamic localization of Scd5-GFP (D) and Prk1-GFP (G) in reference to Pan1-CFP. More than 20 patches were examined in each case, and ~90% of them had similar behaviors as shown. (E and H) Plots of patch fluorescence intensities in Figure 5D (E) and Figure 5G (H) with time. (I) Lifetimes ± SD of Pan1-GFP patches in YMC494 cells transformed with pRS424, pEND3-424, or pSCD5-424. $n \geq 30$ patches. (J) Lifetime of Pan1-GFP patches in wild-type (YMC494) and $scd5^{AAA}$ mutant (YMC499) cells. $n \geq 30$ patches. All scale bars are 4 μm.

arrival of Prk1p suggests that these two proteins are diffused into cytosol after they are phosphorylated by Prk1p.

Consistently, overproduction of End3p and Scd5p, both of which caused marked reduction in phosphorylation of Pan1p by Prk1p (data not shown), dramatically prolonged the patch life of Pan1-GFP to 40 and 45 s, respectively (Figure 6I). The life span of Pan1-GFP patches was also significantly extended in the *scd5*^{AAA} mutant (Figure 6J), in agreement with the above-mentioned observation that Pan1p phosphorylation was hindered in this mutant. In summary, the behaviors of the fluorescent Scd5p and Prk1p in live cells correlate very well with their roles in phosphoregulation of Pan1p.

DISCUSSION

Phosphorylation and dephosphorylation are the most commonly occurring scheme of regulation in a wide variety of biological processes. Pathways like endocytosis, which require recurrent assembly and disassembly of multiprotein complexes at restricted cellular locations, are perhaps best suited to this type of regulation. Our current understanding of phosphoregulation of actin-coupled endocytosis in yeast has been limited to some of the actions of the Prk1p family of kinases. In this report, we reveal that the type 1 phosphatase Glc7p also takes part in this regulatory circuit, counteracting Prk1p in modifying the phosphorylation status, and hence the activity, of the important endocytic protein Pan1p.

Glc7p as the Phosphatase for Pan1p Dephosphorylation

Glc7p is an essential type 1 protein phosphatase localized in the nucleus and the cytosol, and known to participate in diverse cellular processes (Stark, 1996). Although it has recently been implicated in the regulation of actin organization and endocytosis by the finding that it interacts with Scd5p (Chang *et al*., 2002), its exact function in this aspect has remained unexplored. We demonstrated that Glc7p is responsible for modulating the in vivo phosphorylation status of at least two regulatory targets of the Prk1p kinase, i.e., Pan1p and Scd5p, both of which are essential for normal actin organization and endocytosis. The findings that pinpoint Glc7p as the phosphatase to dephosphorylate Pan1p include the phosphorylation level of Pan1p being markedly elevated in Glc7p-depleted cells, the phosphatase being able to dephosphorylate Pan1p in vitro, and the interaction with Scd5p being critical for maintaining the normal steady-state phosphorylation level of Pan1p. Although Glc7p was found to interact with Pan1p directly in a report of a large-scale two-hybrid screen (Uetz *et al*., 2000), we have failed to confirm such interaction in our assays (data not shown).

The role of Glc7p in dephosphorylation of Pan1p is also supported by the functional antagonism between Glc7p and Prk1p. The defects resulted from phosphatase depletion in *glc7-td* cells including actin aggregation, mild delay in endocytosis of uracil permease, and cell lethality, could all be at least partially alleviated by deletion of the kinase gene. As Glc7p is empowered with multifarious cellular functions, it is expected that removal of just one of its antagonistic kinases with a specialized function in actin and endocytosis will not be able to fully compensate for the loss of the phosphatase activity. Nevertheless, the much improved survival of the *prk1*Δ *glc7-td* cells at high temperatures does indicate that the actin- and endocytosis-related dephosphorylation is an important part of the overall Glc7p cellular functions.

Glc7p should be the major protein phosphatase for Pan1p dephosphorylation, because the Pan1p phosphorylation level was not altered in the mutants defective in Ppz1p and Ppz2p (our unpublished data), two other phosphatases that share some overlapping functions with Glc7p (Venturi *et al*., 2000).

The Roles of Scd5p in Phosphoregulation of Pan1p

The key to the mechanism of Pan1p dephosphorylation by Glc7p is the Glc7p targeting factor Scd5p. On one hand, it links the phosphatase to Pan1p by interacting with both Pan1p and End3p. Our results are consistent with the conclusion that Scd5p is essential for maintaining the physiological phosphorylation level of Pan1p by acting as a phosphatase-targeting factor. Scd5p, on the other hand, may also act as a switch in the phosphoregulation of Pan1p, because the phosphorylation status of Pan1p in vivo is dependent on that of Scd5p. When phosphorylation takes place, Prk1p may be obliged to phosphorylate Scd5p first before it can phosphorylate Pan1p, as suggested from the experiment that the nonphosphorylatable Scd5p (Scd5^{AAA}) blocked phosphorylation of Pan1p by overexpressed Prk1p. This mechanism can be interpreted as to ensure the release of Scd5p from the Pan1p–End3p complex in the event of phosphorylation, as the dissociation of Scd5p from the Pan1p–End3p complex is likely required for its binding with Glc7p in the cytosol. The free and phosphorylated Scd5p, in effect, serves as a feedback signal for the process of dephosphorylation.

Therefore, the role of Scd5p in the phosphoregulation of Pan1p during endocytosis is twofold: the patch-localized Scd5p, in complex with Pan1p–End3p, functions as a switch in the event of phosphorylation, whereas the cytoplasmic Scd5p, in complex with Glc7p, acts as a phosphatase targeting factor in the event of dephosphorylation. Of the two roles of Scd5p, only the latter is essential. It has been reported that the cortical localization of Scd5p is not required for its actin and endocytic functions, since these functions remained apparently normal in a cytoplasmically localized Scd5p mutant (Chang *et al*., 2006). This mutant, nevertheless, is expected to be functional as the phosphatase-targeting factor, because it is still able to interact with End3p in the cytosol. The *scd5-*Δ*338* mutant, on the other hand, is temperature sensitive and defective in endocytosis, because the truncated protein is predominantly localized to the nucleus (Henry *et al*., 2002; Chang *et al*., 2006). Consistent with our findings, this mutation could be suppressed by deletion of the kinase gene *PRK1* (Henry *et al*., 2003).

Cycle of Phosphoregulation of Pan1p during Endocytosis

With the identification of the role of the Scd5p–Glc7p phosphatase complex in dephosphorylation of Pan1p, combined with previous discoveries made by other groups, it is now possible to propose a model of a complete cycle of the phosphoregulation of Pan1p during endocytosis (Figure 7): 1) Assembly of the endocytic complex at the site of endocytosis, in which Pan1p is complexed with End3p and Scd5p, together with other coat proteins and present in an unphosphorylated state. 2) Initiation of actin polymerization by the Arp2/3p complex to induce membrane invagination. 3) Vesicle scission and inward movement propelled by actin polymerization. 4) Phosphorylation of Scd5p and Pan1p by Prk1p to disassemble the coat complex. Incorporation of the kinase into the complex at this stage involves Abp1p (Fazi *et al*., 2002), which appears on the Pan1p patches at about same time as Prk1p (Kaksonen *et al*., 2003). The kinase starts by phosphorylating and dissociating Scd5p from Pan1p and End3p, followed by extensive phosphorylation of Pan1p. This presumably will cause a distortion/disrup-

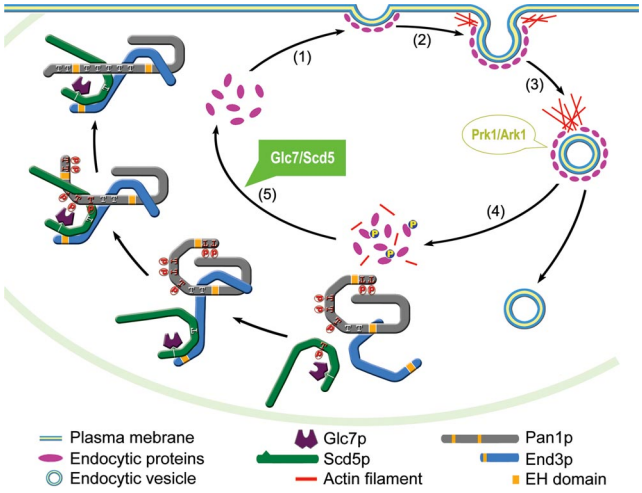

Figure 7. Simplistic model of actin-driven endocytosis in yeast with an emphasis on phosphoregulation of Pan1p by Prk1p and Glc7p. Steps 1 through 4 occur on the cortical patches, and step 5 (dephosphorylation) takes place in the cytosol. See text for detailed description.

tion of the interactions among endocytic coat proteins and a termination of Pan1p-dependent actin polymerization. 5) Dephosphorylation of Pan1p in the cytosol. Phosphorylated Scd5p is released into cytosol, so is phosphorylated Pan1p, which remains to be bound by End3p (Toshima *et al*., 2007). Scd5p is then bound and dephosphorylated by Glc7p, whose binding with Scd5p is unaffected by Prk1p phosphorylation. Dephosphorylation of Pan1p starts by reassociation of Scd5p with End3p. Once it initiates, dephosphorylation of Pan1p is expected to be a self-accelerating process, as the first cluster of phosphor residues to be cleared are likely those located adjacent to the End3p- and Scd5p-binding region (LR2), and dephosphorylation in this region will result in a more secured interaction between Pan1p and Scd5p. This will in turn facilitate the dephosphorylation of other sites located in the LR1 region. Dephosphorylated Pan1p is now once again ready to lead the next round of endocytosis (Figure 7). Glc7p will become detached from the complex probably at the time when dephosphorylated Pan1p and Scd5p begin to interact with other coat proteins. This model also fits well with our live cell imaging data. For example, we observed that Pan1p and Scd5p have similar patch lifetime, and the two proteins appear on, and disappear from, the patches at about same time. The time of Prk1p arrival on the Pan1p patches is also consistent with the concept that Prk1p phosphorylation initiates disassembly of the endocytic coat complex.

Other Considerations

In addition to Pan1p, other endocytic proteins known to be phosphorylated by Prk1p, such as Sla1p, Ent1/2p and Yap1801/2p (Watson *et al*., 2001; Zeng *et al*., 2001; Huang *et al*., 2003), may also be dephosphorylated by the Scd5p-targeted Glc7p. For example, the yeast homologue of mammalian Huntingtin-interacting protein 1R, Sla2p, which contains a single Prk1p phosphorylation motif (Huang *et al*., 2003), has been reported to be involved in interactions with Ark1p and Scd5p (Cope *et al*., 1999; Henry *et al*., 2002). It will be interesting to find out whether Sla2p is phosphoregulated by Prk1p/Ark1p and Glc7p in a similar manner as Pan1p. Sla1p has also been reported to interact with Glc7p (Tu *et al*., 1996; Venturi *et al*., 2000), although we failed to confirm such interaction in our yeast two-hybrid assays. Whether Sla1p could act as a phosphatase-targeting factor and at the same time a substrate, similarly to Scd5p, remains to be clarified.

In mammalian cells, kinases with similar function and property as that of Prk1p have also been identified. The adaptor-associated kinase AAK1 negatively regulates clathrin-mediated endocytosis by phosphorylating the μ2 subunit of the AP2 adaptor protein complex (Conner and Schmid, 2002; Ricotta *et al*., 2002). Interestingly, AAK1 shares with Prk1p not only the extensive kinase sequence homology but also the similar recognition motif (Conner and Schmid, 2002; Ricotta *et al*., 2002). Another mammalian homologue of Prk1p, GAK, also exhibits a similar specificity on the μ2 subunit and plays a regulatory role in endocytosis (Zhang *et al*., 2005). AP2 is known to associate with Eps15, the mammalian counterpart of Pan1p, and such interaction is required for endocytosis (Benmerah *et al*., 1995, 1998). Unlike Pan1p, however, Eps15 contains no AAK1/GAK recognition motifs, and it has yet to be ascertained whether it is subjected to regulation by these kinases. It also remains unknown how the dephosphorylation of AP2 is carried out. The mammalian PP1 has not been demonstrated to be involved in clathrin-mediated endocytosis, despite its vast variety of other known cellular functions through >50 established or putative binding subunits (Cohen, 2002). Therefore, it will be of great interest to identify novel targeting factor(s) of PP1, or other type of phosphatases, with a specific function in clathrin-mediated endocytosis in mammalian cells.

ACKNOWLEDGMENTS

We are grateful to Claire Moore (Tufts University) for providing the pGLC7-degron plasmid (pGLC7n-td-306) and to David Drubin (University of California, Berkeley) for the Pan1-GFP harboring strain DDY3063. We also thank Desmond Dorairajoo and Yong Xiao for helping microscopy and imaging data analysis. We thank Jun Wang and Chong Yun Won for general technical assistance. This work was supported by the Agency for Science, Technology & Research of Singapore. M.C. holds an adjunct faculty appointment from the Department of Biochemistry, Faculty of Medicine, National University of Singapore.

REFERENCES

Benedetti, H., Raths, S., Crausaz, F., and Riezman, H. (1994). The END3 gene encodes a protein that is required for the internalization step of endocytosis and for actin cytoskeleton organization in yeast. Mol. Biol. Cell *5*, 1023–1037.

Benmerah, A., Gagnon, J., Begue, B., Megarbane, B., Dautry-Varsat, A., and Cerf-Bensussan, N. (1995). The tyrosine kinase substrate eps15 is constitutively associated with the plasma membrane adaptor AP-2. J. Cell Biol. *131*, 1831–1838.

Benmerah, A., Lamaze, C., Begue, B., Schmid, S. L., Dautry-Varsat, A., and Cerf-Bensussan, N. (1998). AP-2/Eps15 interaction is required for receptor-mediated endocytosis. J. Cell Biol. *140*, 1055–1062.

Chang, J. S., Henry, K., Geli, M. I., and Lemmon, S. K. (2006). Cortical recruitment and nuclear-cytoplasmic shuttling of Scd5p, a protein phosphatase-1-targeting protein involved in actin organization and endocytosis. Mol. Biol. Cell *17*, 251–262.

Chang, J. S., Henry, K., Wolf, B. L., Geli, M., and Lemmon, S. K. (2002). Protein phosphatase-1 binding to Scd5p is important for regulation of actin organization and endocytosis in yeast. J. Biol. Chem. *277*, 48002–48008.

Cohen, P., Klumpp, S., and Schelling, D. L. (1989). An improved procedure for identifying and quantitating protein phosphatases in mammalian tissues. FEBS Lett. *250*, 596–600.

Cohen, P. T. (2002). Protein phosphatase 1–targeted in many directions. J. Cell Sci. *115*, 241–256.

Conner, S. D., and Schmid, S. L. (2002). Identification of an adaptor-associated kinase, AAK1, as a regulator of clathrin-mediated endocytosis. J. Cell Biol. *156*, 921–929.

Cope, M. J., Yang, S., Shang, C., and Drubin, D. G. (1999). Novel protein kinases Ark1p and Prk1p associate with and regulate the cortical actin cytoskeleton in budding yeast. J. Cell Biol. *144*, 1203–1218.

Dohmen, R. J., Wu, P., and Varshavsky, A. (1994). Heat-inducible degron: a method for constructing temperature-sensitive mutants. Science *263*, 1273–1276.

Duncan, M. C., Cope, M. J., Goode, B. L., Wendland, B., and Drubin, D. G. (2001). Yeast Eps15-like endocytic protein, Pan1p, activates the Arp2/3 complex. Nat. Cell Biol. *3*, 687–690.

Fazi, B., Cope, M. J., Douangamath, A., Ferracuti, S., Schirwitz, K., Zucconi, A., Drubin, D. G., Wilmanns, M., Cesareni, G., and Castagnoli, L. (2002). Unusual binding properties of the SH3 domain of the yeast actin-binding protein Abp *1*, structural and functional analysis. J. Biol. Chem. *277*, 5290–5298.

Feng, Z. H., Wilson, S. E., Peng, Z. Y., Schlender, K. K., Reimann, E. M., and Trumbly, R. J. (1991). The yeast GLC7 gene required for glycogen accumulation encodes a type 1 protein phosphatase. J. Biol. Chem. *266*, 23796–23801.

Francisco, L., Wang, W., and Chan, C. S. (1994). Type 1 protein phosphatase acts in opposition to IpL1 protein kinase in regulating yeast chromosome segregation. Mol. Cell. Biol. *14*, 4731–4740.

He, X., and Moore, C. (2005). Regulation of yeast mRNA 3′ end processing by phosphorylation. Mol. Cell *19*, 619–629.

Henry, K. R., D'Hondt, K., Chang, J., Newpher, T., Huang, K., Hudson, R. T., Riezman, H., and Lemmon, S. K. (2002). Scd5p and clathrin function are important for cortical actin organization, endocytosis, and localization of sla2p in yeast. Mol. Biol. Cell *13*, 2607–2625.

Henry, K. R., D'Hondt, K., Chang, J. S., Nix, D. A., Cope, M. J., Chan, C. S., Drubin, D. G., and Lemmon, S. K. (2003). The actin-regulating kinase Prk1p negatively regulates Scd5p, a suppressor of clathrin deficiency, in actin organization and endocytosis. Curr. Biol. *13*, 1564–1569.

Hisamoto, N., Sugimoto, K., and Matsumoto, K. (1994). The Glc7 type 1 protein phosphatase of *Saccharomyces cerevisiae* is required for cell cycle progression in G2/M. Mol. Cell. Biol. *14*, 3158–3165.

Huang, B., Zeng, G., Ng, A. Y., and Cai, M. (2003). Identification of novel recognition motifs and regulatory targets for the yeast actin-regulating kinase Prk1p. Mol. Biol. Cell *14*, 4871–4884.

Kaksonen, M., Sun, Y., and Drubin, D. G. (2003). A pathway for association of receptors, adaptors, and actin during endocytic internalization. Cell *115*, 475–487.

Kaksonen, M., Toret, C. P., and Drubin, D. G. (2005). A modular design for the clathrin- and actin-mediated endocytosis machinery. Cell *123*, 305–320.

Kaksonen, M., Toret, C. P., and Drubin, D. G. (2006). Harnessing actin dynamics for clathrin-mediated endocytosis. Nat. Rev. Mol. Cell Biol. *7*, 404–414.

Merrifield, C. J. (2004). Seeing is believing: imaging actin dynamics at single sites of endocytosis. Trends Cell Biol. *14*, 352–358.

Ricotta, D., Conner, S. D., Schmid, S. L., von Figura, K., and Honing, S. (2002). Phosphorylation of the AP2 mu subunit by AAK1 mediates high affinity binding to membrane protein sorting signals. J. Cell Biol. *156*, 791–795.

Stark, M. J. (1996). Yeast protein serine/threonine phosphatases: multiple roles and diverse regulation. Yeast *12*, 1647–1675.

Sun, Y., Martin, A. C., and Drubin, D. G. (2006). Endocytic internalization in budding yeast requires coordinated actin nucleation and myosin motor activity. Dev. Cell *11*, 33–46.

Tang, H. Y., and Cai, M. (1996). The EH-domain-containing protein Pan1 is required for normal organization of the actin cytoskeleton in *Saccharomyces cerevisiae*. Mol. Cell. Biol. *16*, 4897–4914.

Tang, H. Y., Munn, A., and Cai, M. (1997). EH domain proteins Pan1p and End3p are components of a complex that plays a dual role in organization of the cortical actin cytoskeleton and endocytosis in *Saccharomyces cerevisiae*. Mol. Cell. Biol. *17*, 4294–4304.

Tang, H. Y., Xu, J., and Cai, M. (2000). Pan1p, End3p, and S1a1p, three yeast proteins required for normal cortical actin cytoskeleton organization, associate with each other and play essential roles in cell wall morphogenesis. Mol. Cell. Biol. *20*, 12–25.

Toshima, J., Toshima, J. Y., Duncan, M. C., Cope, M. J., Sun, Y., Martin, A. C., Anderson, S., Yates, J. R., 3rd, Mizuno, K., and Drubin, D. G. (2007). Negative regulation of yeast Eps15-like Arp2/3 complex activator, Pan1p, by the Hip1R-related protein, Sla2p, during endocytosis. Mol. Biol. Cell *18*, 658–668.

Toshima, J., Toshima, J. Y., Martin, A. C., and Drubin, D. G. (2005). Phosphoregulation of Arp2/3-dependent actin assembly during receptor-mediated endocytosis. Nat. Cell Biol. *7*, 246–254.

Tu, J., and Carlson, M. (1994). The GLC7 type 1 protein phosphatase is required for glucose repression in *Saccharomyces cerevisiae*. Mol. Cell. Biol. *14*, 6789–6796.

Tu, J., and Carlson, M. (1995). REG1 binds to protein phosphatase type 1 and regulates glucose repression in *Saccharomyces cerevisiae*. EMBO J. *14*, 5939–5946.

Tu, J., Song, W., and Carlson, M. (1996). Protein phosphatase type 1 interacts with proteins required for meiosis and other cellular processes in *Saccharomyces cerevisiae*. Mol. Cell. Biol. *16*, 4199–4206.

Uetz, P. *et al*. (2000). A comprehensive analysis of protein-protein interactions in *Saccharomyces cerevisiae*. Nature *403*, 623–627.

Venturi, G. M., Bloecher, A., Williams-Hart, T., and Tatchell, K. (2000). Genetic interactions between GLC7, PPZ1 and PPZ2 in saccharomyces cerevisiae. Genetics *155*, 69–83.

Volland, C., Urban-Grimal, D., Geraud, G., and Haguenauer-Tsapis, R. (1994). Endocytosis and degradation of the yeast uracil permease under adverse conditions. J. Biol. Chem. *269*, 9833–9841.

Wach, A., Brachat, A., Alberti-Segui, C., Rebischung, C., and Philippsen, P. (1997). Heterologous HIS3 marker and GFP reporter modules for PCR-targeting in *Saccharomyces cerevisiae*. Yeast *13*, 1065–1075.

Watson, H. A., Cope, M. J., Groen, A. C., Drubin, D. G., and Wendland, B. (2001). In vivo role for actin-regulating kinases in endocytosis and yeast epsin phosphorylation. Mol. Biol. Cell *12*, 3668–3679.

Wek, R. C., Cannon, J. F., Dever, T. E., and Hinnebusch, A. G. (1992). Truncated protein phosphatase GLC7 restores translational activation of GCN4 expression in yeast mutants defective for the eIF-2 alpha kinase GCN2. Mol. Cell. Biol. *12*, 5700–5710.

Wendland, B., and Emr, S. D. (1998). Pan1p, yeast eps15, functions as a multivalent adaptor that coordinates protein-protein interactions essential for endocytosis. J. Cell Biol. *141*, 71–84.

Wendland, B., Steece, K. E., and Emr, S. D. (1999). Yeast epsins contain an essential N-terminal ENTH domain, bind clathrin and are required for endocytosis. EMBO J *18*, 4383–4393.

Zeng, G., and Cai, M. (1999). Regulation of the actin cytoskeleton organization in yeast by a novel serine/threonine kinase Prk1p. J. Cell Biol. *144*, 71–82.

Zeng, G., Yu, X., and Cai, M. (2001). Regulation of yeast actin cytoskeleton-regulatory complex Pan1p/Sla1p/End3p by serine/threonine kinase Prk1p. Mol. Biol. Cell *12*, 3759–3772.

Zhang, C. X., Engqvist-Goldstein, A. E., Carreno, S., Owen, D. J., Smythe, E., and Drubin, D. G. (2005). Multiple roles for cyclin G-associated kinase in clathrin-mediated sorting events. Traffic *6*, 1103–1113.